

# THE EXTENDED NARROW LINE REGION OF 3C 299<sup>1</sup>

Carlos Feinstein<sup>2</sup>

Observatorio Astronómico, Paseo del Bosque, 1900 La Plata, Argentina

F. Duccio Macchetto<sup>3</sup>, André R. Martel, William B. Sparks  
Space Telescope Institute, 3700 San Martin Drive, Baltimore, MD 21218

Patrick J. McCarthy

The Observatories of the Carnegie Institution of Washington, 813 Santa Barbara Street,  
Pasadena, CA 91101

## ABSTRACT

We present results of HST observations of the radio galaxy 3C 299. The broad-band F702W (R) and F555W (V) images (WFPC2/PC) show an elliptical galaxy, with a comet-like structure extending to the NE in the radio jet direction. The [OIII] $\lambda$ 5007 emission line map, shows a bi-conical structure centered on the nucleus, that overlaps the structure found in the broad-band filters. The radio core coincides with the center of the bi-conical structure and the radio axes are aligned with the direction of the cones. These data show clear evidence of a strong interaction between the radio jet and the NE morphology of the galaxy.

We show evidence that this NE region is an ENLR; the line-ratio diagnostics show that models involving gas shocked by the radio-jet plus ionization from a precursor HII region, produced itself by the ionizing photons of the postshocked gas on the preshocked gas provide a good match to the observations.

We investigate the spatial behavior of the ionizing parameter  $U$ , by determining the [OIII]/[OII] line ratio which is sensitive to the change of the ionization parameter, and trace its behavior over the ENLR along the radio jet direction. We find that [OIII]/[OII] does not follow a simple dilution model, but rather that it is approximately constant over a large range of distance from the nucleus thus requiring a local source of ionization which seems to be compatible with the shock models driven by the radio jet.

---

<sup>1</sup>Based on observations made with the NASA/ESA *Hubble Space Telescope*, which is operated by the Association of Universities for Research in Astronomy, Inc, under NASA contract NAS 5-26555

<sup>2</sup>Member of Carrera del Investigador Conicet, Argentina

<sup>3</sup>On assignment from the Space Science Department of ESA

*Subject headings:* AGN - Radio Galaxies - Jets

## 1. Introduction

Over the last few years we have undertaken a systematic survey of extragalactic radio sources (de Koff et al. 1996; Martel et al. 1998a,b ; McCarthy et al. 1997) in the 3CR Catalogue (Bennett 1962a,b; Spinrad et al. 1985) using WFPC2 on HST. These data allow us to investigate the relationships between the radio and optical morphologies in a complete sample of powerful radio galaxies. Imaging of nearby Seyfert galaxies with HST, such as Mrk 3, Mrk 6, Mrk 573, NGC 1068, NGC 2992 and NGC 4151, (Capetti et al., 1995a, 1995b, 1996, 1997; Winge et al. 1997; Allen et al. 1998,1999; Axon et al, 1998) has shown an intimate connection between the radio structure and the extended NLR (ENLR). These studies show that the interaction of the radio jet with the ISM is the main source of UV photons that ionize the ENLR in Seyfert galaxies. We wish to investigate whether this scenario is also applicable to the high-power radio sources and in particular the radio galaxy 3C 299.

This galaxy is a FR II and one of the most asymmetric double-lobed radio AGNs (Liu et al. 1992) not only because of the significantly different distance between the nucleus and each of the lobes but also in terms of lobe flux and lobe length. The radio morphology consists of a compact radio-core and two lobes separated by  $11''$  at PA  $\sim 63^\circ$ . The NE lobe is larger ( $\sim 1.5''$ ) and brighter (441.6 mJy at 8.4 Ghz, Akujor et al. 1995) than the SW lobe ( $\sim 0.7''$  and 20.1 mJy). The core does not appear to be located at the geometrical center of the lobes; it is  $3''$  nearer the NE lobe (Liu et al 1991). For some time, due to this large asymmetry, the NE lobe itself was believed to be the central component of a compact steep-spectrum source (CSS). But when the SW component was found by Laing (1981), and the central component by Liu & Pooley (1991) and van Breugel et al (1992), the true picture of 3C 299 as a double-lobed radio AGN fully emerged.

At optical wavelengths this galaxy appears to be a low-redshift analogue of the high redshift ( $z>1$ ) radio galaxies studied by McCarthy et al. (1995) since its optical continuum emission is elongated and aligned with the radio source axis. The emission lines have a complex morphology and kinematics, with the [OIII] $\lambda$ 5007 line offset from the continuum peak (McCarthy et al. 1996).

In this paper we discuss the complex morphology of 3C 299 shown by the high spatial HST resolution images and we compare it with the radio data. We investigate the physical

conditions of the ENLR through ground-based long-slit spectroscopy data and show that the ionization parameter is roughly constant throughout the ENLR.

We conclude by showing that a simple mechanism to provide the required ionizing photons are shocks triggered by the interaction of the radio jet with the local ISM (Capetti et al. 1995a, 1995b), as in the case of the lower redshift Seyfert galaxies.

## 2. Observations and data analysis

The HST/WFPC2 observations of 3C 299 were taken as part of the 3CR Snapshot Survey (PI: W. B. Sparks) which was conducted in cycles 4 to 7, in the F555W and F702W broad bands as well as narrow emission line bands. (de Koff et al. 1996; Martel et al. 1998a,b; McCarthy et al. 1997). The 3C 299 images were obtained with the WFPC2/PC and the F702W filter in May 1995 and the F555W filter in September 1996. Narrow-band images with the WFPC2/WF2 and the FR680N ramp filter were taken in August 1995. Table 1 shows the observation log.

At a redshift of  $z=0.367$ , the galaxy is at a distance of 1.3 Gpc with a projected linear scale of 4.7 kpc/arcsec (assuming  $H_0=65$  km sec $^{-1}$  Mpc $^{-1}$  and  $q_0 = 0.5$ ). The WFPC2/PC scale is 0".0455/pixel and for the WFPC2/WF2 the scale is 0".0996/pixel, and therefore, the physical scales for the images are 213 parsecs/pixel for the PC mode and 471 parsecs/pixel for the WF2 mode.

The reduction procedure for the F702W filter data, which is close to Cousins R filter, is fully discussed in Martel et al. (1998b). This reduction includes the standard WFPC2 pipeline processing and cosmic-ray removal. The data reduction was carried out using IRAF and the STSDAS package. At the redshift of 3C 299, the F702W data includes the H $\beta$  and [OIII] emission lines. The F555W filter data, which is closer to Johnson V, was reduced in the same way and then registered and added to produce one final image with higher S/N. Due to the redshift the F555W image includes the flux from the emission lines of [OII], [NeIII], H $\delta$  and H $\gamma$ . In what follows we will define F702W as R, and F555W as V. The FR680N is a narrow-band ramp filter, which given the redshift of the galaxy and its position on the CCD, produces an [OIII]  $\lambda 5007$  image. These images were reduced as described above and the final image was re-scaled to the resolution of the WFPC2/PC.

The F702W and F555W filter data were flux-calibrated using values for the inverse sensitivities (PHOTFLAM) of  $1.866 \times 10^{-18}$  ergs cm $^{-2}$   $\text{\AA}^{-1}$  DN $^{-1}$ ,  $3.491410 \times 10^{-18}$  cm $^{-2}$   $\text{\AA}^{-1}$  DN $^{-1}$ , and zero-points for the Vega system of  $M_{Photzpt}=-21.85$ ,  $M_{Photzpt}=-21.07$  respectively. Non-rotated images were used for these flux calibrations. The FR680N filter

was calibrated using the ramp filter calculator (Biretta et al, 1996). An approximate coordinate frame for the WFPC2 data is provided by the image header information, based on the HST guide stars. The accuracy at the coordinates is approximately  $1''$  (Biretta et al. 1996).

Images obtained with different filters were registered to a common frame using cross-correlation of the brighter elliptical structures. To derive the spatial shift between the broad-band filters images and the FR680N image, we used the filamentary NE structure, since this structure is well defined and bright in both filters. The sky background in each image was determined through the statistical analysis of a 3-sigma clipping of the average background value in several regions in each of the images.

To compare with radio data, we used the observations from Leahy (1997), obtained with MERLIN at 1534 MHz and posted on the DRAGN's Web site maintained by Leahy, Bridle, & Strom R., at the Jodrell Bank Observatory.

### 3. Results

The optical broad-band images possess a complex morphology (Fig. 1). The V and R images show a central elliptical structure, with two bright cusps separated by an absorption lane,  $\sim 0''.3 \times 1''.4$  (i.e.  $1.2 \times 5.7$  kpcs). To the NE, separated by 1.4 arcsec, there is an extended filamentary structure. This region shows a shell-like structure with bright, sharp but resolved filaments enclosing what appears to be a bubble of lower intensity emission.

We found that the elliptical is well fitted by an  $r^{1/4}$  surface brightness profile. From the isophotal fitting, the position of the nucleus is found to be hidden behind the central absorption lane. From the V-R map, we derive values for the color index. The elliptical galaxy has a color index of  $1.0 < (V-R) < 1.33$ , which is compatible with the values from Rönnbach et al. (1996) for the stellar population of a elliptical galaxy at the redshift of 3C 299. The faint region between the brighter cusps has  $1.53 < (V-R) < 2.0$  and these values are also compatible with a stellar population reddened by a dust lane.

The FR680N filter shows a rather different picture, since the data is dominated by emission in the  $[\text{OIII}]\lambda 5007$  line. The image (Fig. 2) shows a bi-conical structure of ionized oxygen, bright and large to the NE and faint and small to the SW. The NE cone has a full opening angle of 45 degrees, from PA  $30^\circ$  to PA  $75^\circ$ . The geometry and the brightness intensity (in comparison with the broad-band filters data) of this structure in the  $[\text{OIII}]\lambda 5007$  emission-line data indicates that this flux came from the extended NLR (ENLR). This is consistent with the previous studies of McCarthy et al. (1995, 1996). The

shape of the NE bright lobe in this data is the same as that in the broad-band filters. Since there is almost no continuum emission (as the elliptical galaxy profile vanished) in the NE bright lobe, the broad-band filter morphology is dominated by the line-emission, therefore we used it to register the broad-band data to the narrow-band data.

Using a bi-dimensional cross-correlation technique (CROSSCOR task in IRAF/STSDAS) we find that the center of the bi-conical structure coincides with the geometric center of the elliptical galaxy. Fig 3 shows the superposition of the [OIII] data over the R data; note that the NE structure coincides with the line emission. If we make the obvious assumption that the center (nucleus) of the elliptical galaxy is coincident with the radio core, it follows that the radio axis (PA  $63^\circ$ ) is reasonably well aligned with the emission-line region (PA  $52^\circ$ ). Furthermore the NE radio lobe is clearly related to the ENLR in the [OIII] image and with the large filamentary shell-like structure that is seen in the broad-band filters (Fig. 4a,b).

We derived values for the physical conditions of the emitting gas by analyzing and measuring line-emission ratios of the optical spectrum of McCarthy et. al. (1996), taken with the Lick 3 m telescope. The  $2''$  slit was positioned along the radio source axis (P.A.  $\sim 70^\circ$ ), thus crossing the ENLR and covering a wavelength range from 4600 to 7400 Å. The McCarthy et al. data shows that the peak of the [OIII] and  $H\beta$  lines are offset from the continuum (see Fig 5 for a plot of this spectrum in the range from 6300 to 7400 Å). Therefore the maximum of the line emission lies outside the nucleus and towards the ENLR. The high excitation line HeII  $\lambda$  4686 is present and shows a similar behavior with extensions towards the ENLR.

One interesting point is to understand what dominates the flux in the broad-band images at the ENLR. For the F555W data the [OII] $\lambda$ 3727 and the [NeIII] $\lambda$ 3869 are present, and there is no observable continuum in the ENLR spectrum. Since the [NeIII] $\lambda$ 3869 emission is low (<30%) compared to the [OII] $\lambda$ 3727 and also the [OII] $\lambda$ 3727/[NeIII] $\lambda$ 3869 ratio is quite constant over the entire ENLR, it is possible to use the broad-band F555W image as a good estimator of the [OII] $\lambda$ 3727 emission. We used this image, to derive surface brightness profiles and to determine the behavior of the [OIII]/[OII] ratio as an estimate of the spatial behavior of the ionizing parameter ( $U$ ). In Fig. 6 we show the [OIII] and [OII] intensities as a function of distance from the nucleus along the NE radio jet, as well as a plot of the [OIII]/[OII] ratio. The [OII] flux profile includes the contribution from the stellar population of the elliptical galaxy to a distance of about 1 arcsec from the nucleus, where the  $r^{1/4}$  profile vanishes. Therefore, from  $1''$  to  $3''.2$ , the measured flux arises only from ENLR emission lines.

The low amount of contamination of [NeIII] emission in the [OII] data does not affect

the validity of the [OIII]/[OII] ratio. Models such of Dopita et al. 1995, show that the [NeIII] emission follows the trend of the [OIII] emission as the effect of the precursor become more important. Sophisticated photoionization models such as those at Binnete et al. (1996) show a relation between the [NeIII] and [OIII] emission. Therefore, the properties of the [OIII]/[OII] as the tracer of the ionization parameter  $U$  are not affected by the low amount of [NeIII] emission.

The typical error for the [OIII] plot is  $\sigma = \pm 0.7$  for a reference flux of 4  $DN$  calculated with the Extend Exposure Time Calculator (Biretta et al. 1996) and taking into account two pixel binning. For the [OII] plot,  $\sigma = \pm 0.3$  for a 2  $DN$  flux and 8 pixel binning to match the spatial resolution of the upper plot (WF to PC resolution). The errors of the [OIII]/[OII] plot are a combination of the errors of the two upper plots and for example, a reference flux of 5  $DN$  has a maximum error of  $\sigma = \pm 0.9$ , calculated as the large departure from the combination of fluxes and errors of the [OIII] and [OII] profiles.

#### 4. Discussion

Our optical data shows that there is a close morphological relationship between the [OIII] ENLR and the radio emission of the NE lobe. It is interesting to investigate the possible physical scenario for this close relationship. Taylor et al. (1992) proposed that fast bowshocks resulting from the interaction of the radio jet and the ISM were the source of ionizing photons of the emission-line gas. Capetti et al. (1995a, 1995b, 1996, 1997) and Winge et al. (1997) were the first to show that this mechanism best explains the optical emission in the NLR in nearby Seyfert galaxies (Mrk 3, Mrk 6, Mrk 573, NGC 1068, NGC 4151 and NGC 7319). Recently, this work has been confirmed by Aoki et al. (1999) and Kukula et al. (1999).

Dopita & Sutherland (1995a,b) have modeled in detail the ionization of the ENLR by shocks. In one scenario which has been shown to work for Seyfert galaxies, the radio jet interacts with the local interstellar medium and shocks the gas. In this scenario, the hot postshock plasma gas produces photons that can diffuse upstream and downstream of the jet. Photons diffusing upstream can encounter the preshocked gas and produce an extensive precursor HII region, while those traveling downstream will influence the ionization and temperature structure of the recombination of the shock.

This scenario appears very attractive in explaining the morphology of the radio and optical data in 3C 299. To check the validity of this interpretation, we derived values for the physical conditions of the emitting gas by measuring and analyzing the line-emission ratios from the optical spectrum of McCarthy et al. (1996). In Table 2 we list the spatial

behavior of the He II  $\lambda$  4686/H $\beta$  and [OIII]  $\lambda$ 5007/H $\beta$  ratios derived from that spectrum. Figure 7 is the plot of the measure line-ratio at 3.6'' (from the nucleus) over the models of Dopita et al. (1995a), it is clear that the model which includes a high-speed shock ( $\sim$  400 km/sec) plus a precursor HII region photoionization (produced by photons traveling upstream from the shock) fits the observations rather well over the entire ENLR. The values of Table 2 are also fairly constant (within the errors) showing that physical conditions are similar over the jet path.

Another way to check the shock scenario is to explore the spatial behavior of the ionization condition of the gas by estimating the ionization parameter  $U$ . This parameter is defined as  $U = Q/4\pi r^2 c N_e$ , where  $Q$  is the rate at which ionizing photons are emitted from a point source towards a gas cloud with electron density  $N_e$  and distance  $r$  from the ionizing source. If we consider the galactic nucleus to be the ionizing source, as the distance from the nucleus increases for a constant  $N_e$ , the parameter  $U$  will decrease and change the ionization condition of the gas. This change will be reflected in the values of the emission-line ratios (eg. [OIII]/[OII]). However, this parameter will have a very different behavior if the density changes or if there is another source of ionizing photons (such as shocks produced by the radio jet) or a combination of both (from the nucleus and local).

The two brighter peaks in the flux profiles of both [OIII] and [OII], at 1.7'' and 2.4'' from the nucleus arise from the bright filaments of the shell-like structure. Note that both profiles have a similar shape. The [OIII]/[OII] line ratio is rather high from 1.6'' to 2.6'' at the position of these filaments. As noted above this line ratio is strongly dependent on the ionization parameter  $U$ . If there is no local source of ionizing photons, due to geometrical dilution of the ionizing radiation field we expect  $U \sim N_e^{-1} r^{-2}$ . To produce a constant value for  $U$  the electron density should also follow an  $r^{-2}$  law.

Wellman et al. (1996) using radio data for 14 radio-galaxies and 8 radio-loud quasars obtained an estimate of the lobe magnetic field and the lobe speed propagation. From these parameters, they derived an estimate for the ambient gas density in the vicinity of the radio lobe, for the galaxies in their sample using the equation for ram pressure confinement. They found that the ambient gas density can be fitted with a modified King density profile. In particular in our region of interest, within the inner 11  $h^{-1}$  kpc, the density still falls in the flat part of the density distribution, as the core radius of this King profile is 50 (or 100 depending on the model)  $h^{-1}$  kpc. From these, it seems extremely unlikely that the ambient density can vary as  $r^{-2}$ , as would be required to keep the ionization parameter constant in the case that the only source of ionizing photons is the nuclear source. We therefore exclude that ionization by the nuclear source alone can be responsible for the observed ionization of the ENLR lobe.

Similar physical properties of the ENLR, namely a rather constant value for  $U$ , has been reported for some nearby Seyfert 2 galaxies. Capetti et al (1995a), Kukula et al. (1999) show a similar result for Mrk 3, where the radio jets and the optical emissions are very closely associated. In Mrk 6, Capetti et al. (1995b) show that there is also evidence for a transverse ionization structure to the south where the radio jet and the emission lines are co-spatial. In the case of Mrk 573 (Capetti et al. 1996), the ratio  $[OIII]/[OII]$  indicates that the ionization parameter actually increases with radius. These examples provide strong evidence for the scenario where line-emitting gas in the ENLR is compressed by shocks and causes the line emission to be highly enhanced in the region in which this interaction occurs. We can also compare 3C 299 to NGC 1068, one of the closest Seyfert 2 galaxies with a bright radio source and a prominent radio jet which terminates in a extended radio-lobe. For NGC 1068, Capetti et al. (1997) found that the geometrical dilution model of the nuclear radiation field cannot explain the high excitation core formed by the brightest knots of the NLR. An increase (3-4 higher) of the ionization parameter is also observed at a distance of  $\sim 4''$  from the nucleus, where the radio outflow changes its morphology from jet-like to lobe-like. This could be easily explained if there is a density increase where the jet enters the lobe, presumably due to the compression of the backflowing radio cocoon at the jet working surface.

In the case of 3C 299, morphology arguments i.e. the extent and filamentary nature of the ENLR, the structure of the ENLR and its association to the radio-lobe, as well as physical arguments, i.e. the value of the emission-line ratios  $HeII\lambda 4686/H\beta$  and  $[OIII]\lambda 5007/H\beta$  compared to the models of Dopita et al. (1995a) and the constant value for the ionization parameter  $U$ , which does not follow the dilution of the ionizing radiation field for a central source of UV photons, strongly support the same scenario, namely that the ENLR is a product of the interaction of the radio-lobe with the ISM gas.

In contrast to the nearby galaxies, 3C 299 has an intermediate redshift ( $z=0.367$ ), and its ENLR is considerably larger ( $\sim 12$  Kpcs). Best et al. (1996,1998,1999), have carried out deep spectroscopic observations of a number of powerful radio galaxies with redshift  $z \sim 1$  and show that the passage of the radio jet induces shocks through the host galaxy and plays a key role in producing the emission-line gas properties of these objects. Thus the physical connection between the radio jet and the ENLR appears to be at work not only for nearby galaxies, but also for those at higher redshifts. This could provide an explanation for the “alignment effect” found by McCarthy et al. (1987), for high-redshift radio galaxies.

## 5. Summary

We have shown that the elliptical galaxy 3C 299, has a prominent dust lane and bi-conical extended emission line morphology that is similar to those of some lower redshift Seyfert galaxies.

We found that the NE radio radio-lobe lies within the shell-like structure of the ENLR, suggesting a physical connection between the jet and the ENLR. We tested the scenario where the radio jet compresses and shocks the interstellar gas thus producing the observed morphology. From the spectra of McCarthy et al. (1996) we compared the line ratio behavior of the ENLR with the models of Dopita et al. (1995a). From these models we found that the observed spectrum is compatible with gas shocked by the radio jet plus ionization from a precursor HII region, produced by the ionizing photons on the preshocked gas. We also investigated the spatial behavior of the ionizing parameter  $U$ , by determining the [OIII]/[OII] line-ratio which is sensitive to the change of the ionization parameter, and we traced its behavior over the ENLR along the radio jet direction. We found that the [OIII]/[OII] ratio does not follow a simple dilution model, but rather that it is approximately constant over a large area (3 " from the nucleus,  $\sim 12$  kpc ) thus requiring a local source of ionization, and we found that shock models driven by the radio jet, provide the necessary ionizing flux.

Therefore, because of morphology arguments (the NE lobe is locate at the ENLR), physical arguments (the emission-line ratios are consistent with a shock plus an HII precursor region) and the constant value of the ionization parameter (which does not follow the dilution of the ionizing radiation field for a central source of photons), we conclude that the ENLR of 3C 299 is the result of the interaction of the radio jet with the ISM gas.

C.F. acknowledges the support from the STScI visitor program. The Fundacion Antorchas (Argentina) provided partial financial support of this work. We are very grateful to Mark G. Allen for providing us the emission-line diagnostic models for a shock plus an HII region precursor.

## REFERENCES

- Akujor, C.E., Garrington, S.T. 1995, AAS, 112,235  
Allen, M. G., PhD Thesis, 1998, Australian National University  
Allen, M. G., Dopita, M. A., Tsevtanov, Z. I., Sutherland, R. S. 1999, ApJ, 511, 686  
Aoki, K., Kosugi, G., Wilson, A. S., Yoshida, M. 1999, ApJ, in press  
Best, P. N., Longair, M. S., Röttgering, H. J. A. 1996, MNRAS, 280, L9

- Best, P. N., Carilli, C. L., Garrington, S. T., Longair, M. S., Röttgering, H. J. A. 1998, MNRAS, 299, 357
- Best, P. N., M. S., Röttgering, H. J. A., Longair, M. S. 1999, MNRAS, submitted
- Binette, L., Wilson, A.S., Storchi-Bergmann, T. 1996, A&A, 312, 365
- Biretta, J.A. et al. 1996, WFPC2 Instrument Handbook, Version 4.0, Space Telescope Science Institute.
- Capetti, A., Macchetto, F.D., Axon, D.J., Sparks, W.B., Boksenberg, A. 1995, ApJ, 448, 600
- Capetti A., Axon, D.J., Kukula, M., Macchetto, D.F., Pedlar, A., Sparks, W.B., Boksenberg, A. 1995b, ApJ, 454, L85
- Capetti, A., Axon, D.J., Macchetto, F.D., Sparks, W.B., Boksenberg, A. 1996 ApJ, 469, 554
- Capetti, A., Axon, D.J., Macchetto, F.D. 1997, ApJ, 487, 560
- de Koff, S., Baum, S.A., Sparks, W. B., Biretta, J., Golombek, D., Macchetto D. F., McCarthy, P., Miley G. K. 1996 ApJS, 107, 621
- de Vries, W. H., O’dea, C. P., Baum, S. A., Sparks, W. B., Biretta, J., de Koff, S., Golombek, D., Lehnert, M. D., Macchetto, F. McCarthy, P., Miley, G. K. 1997, ApJS, 110, 191
- Dopita, M.A., Sutherland, R. 1996a, ApJ, 455, 468
- Dopita, M.A., Sutherland, R. 1996b, ApJS, 102, 161
- Falcke, H., Wilson, A., Simpson, C. 1998, ApJ, 502, 199
- Kukula, M. J., Ghosh, T., Pedlar, A., Schilizzi, R. T., Space Telescope Preprint Series No 1326
- Leahy, J.P. 1997, private communication
- Liu R., Pooley, G., Riley, J.M. 1991, MNRAS, 253, 669
- Liu R., Pooley, G., Riley, J.M. 1992, MNRAS, 257, 545
- Martel, S. A., Sparks, W. B., Macchetto, F.D., Baum, S.A., Biretta, J. A., Golombek D., McCarthy, P. J., de Koff, S., Miley, G. K. 1998a, AJ, 115, 1348
- Martel, A. R., Baum, S. A., Sparks, W. B., Wyckoff, E., Biretta, J. A., Golombek, D., Macchetto, F.D., de Koff, S., McCarthy, P. J. 1998b, ApJS, in press
- McCarthy, P.J., van Breugel, P. J., Spinrad, H., Djorgovski, S. 1987, ApJ, 321, L29
- McCarthy, P.J., Spinrad, H., Van Breugel, P. J. 1995, ApJS, 99, 27

- McCarthy, P.J., Baum, S., Spinrad, H. 1996, ApJS, 106, 281
- McCarthy, P., J., Miley, G., K., De Koff, S., Baum, S., A., Sparks, William B., Golombek, D., Biretta, J., Macchetto, D.F. 1997, ApJS, 112, 415
- Riley, J.M., Pooley G.G. 1975, Mem. R. Astr. Soc, 105
- Rönback, J., Van Groningen, E., Wanders, I., Örndahl, E. 1996, MNRAS, 283, 282
- Taylor, D., Dyson, J., Axon, D.J. 1992, MNRAS, 255, 35
- van Breugel, W. J. M Fanti, C.; Fanti, R., Stanghellini, C., Schilizzi, R. T., Spencer, R. E 1992, A&A, 256, 56
- Wellman, G. F., Daly, R., Wan, L. 1996, ApJ, 480, 96
- Winge, C., Axon, D.J., Macchetto, F.D., Capetti, A. 1997, ApJ, 487, 121

## Figure Captions

**Fig 1a** F702W (R) image of 3C 299. N is at the top, E is to the left.

**Fig 1b** F555W (V) image of 3C 299.

**Fig 2** [OIII] $\lambda$ 5007 image. The extended-narrow line region shows the bi-conical structure. It is centered on the galaxy nucleus and is bright and extended to the NE.

**Fig 3** Overlap between the [OIII] and the R filter images. Note that the NE structure consists mostly of line emission.

**Fig 4a** Overlap of the radio map at 1450 MHz with the R image.

**Fig 4b** Overlap of the radio map at 1450 MHz with the [OIII] image.

**Fig 5** Long-slit spectrum taken by McCarthy et al. (1996). Note that the peaks of the emission lines are offset from the continuum. Wavelength is redshift corrected.

**Fig 6** Flux profiles ( $DN$  units) of [OIII], [OII] and [OIII]/[OII], as a function of distance from the nucleus along the radio jet. See text for discussions of errors bars.

**Fig 7** Plot of the emission-line ratios over the models of shock + precursor of Dopita et al. (1995). Models are for shock velocities of 200,300 and 500 km/sec and magnetic parameter  $B/n^{1/2}$  of 0,1,2 and 4  $\mu G cm^{3/2}$  respectively.

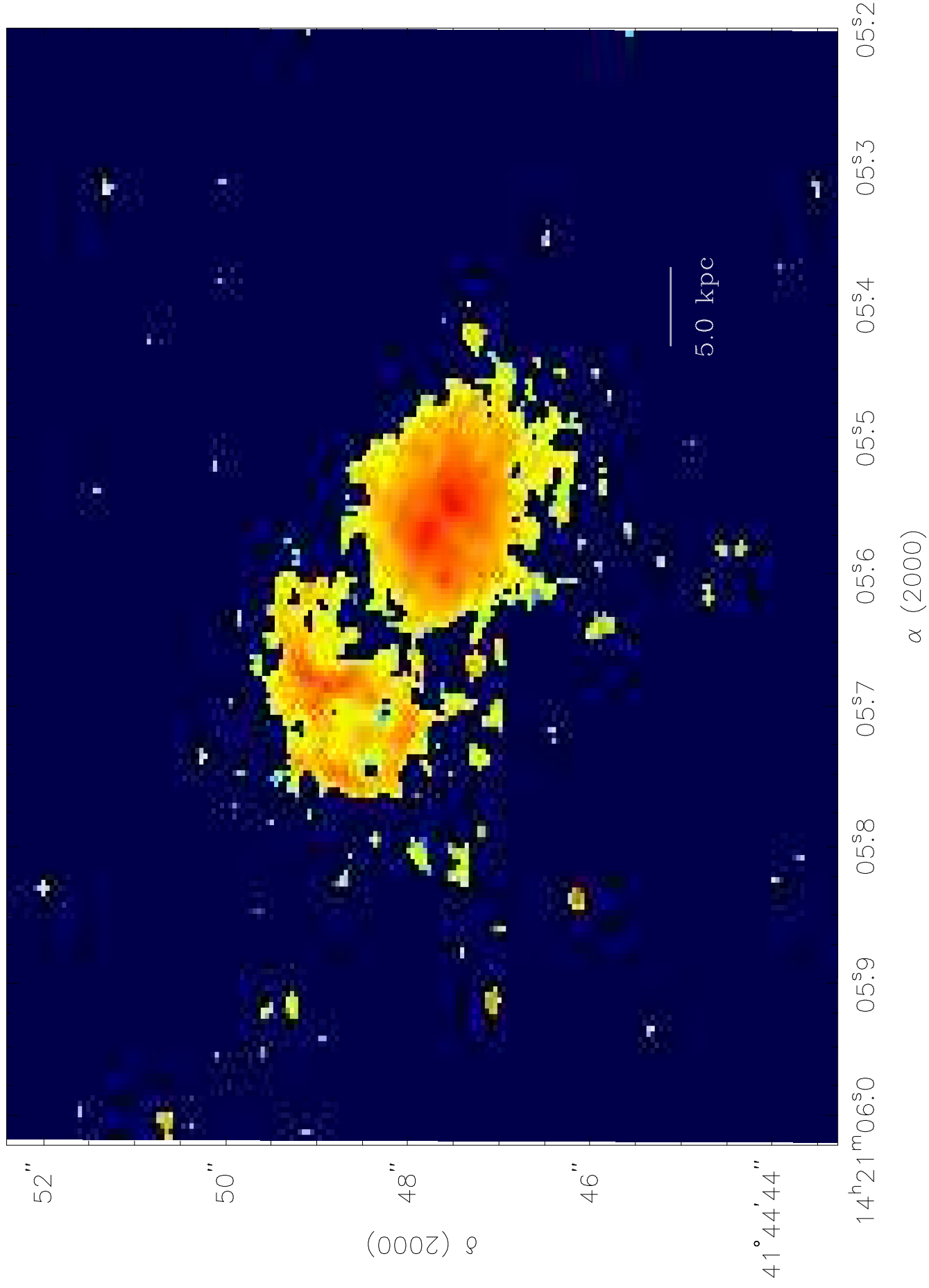
Table 1: Log of observations

Filter Name	Em. Lines	Exp. time sec	Date
F702W		300	May 1995
FR680N	[OIII]	300	Aug. 1995
FR680N	[OIII]	300	Aug. 1995
F555W		300	Sep. 1996
F555W		300	Sep. 1996

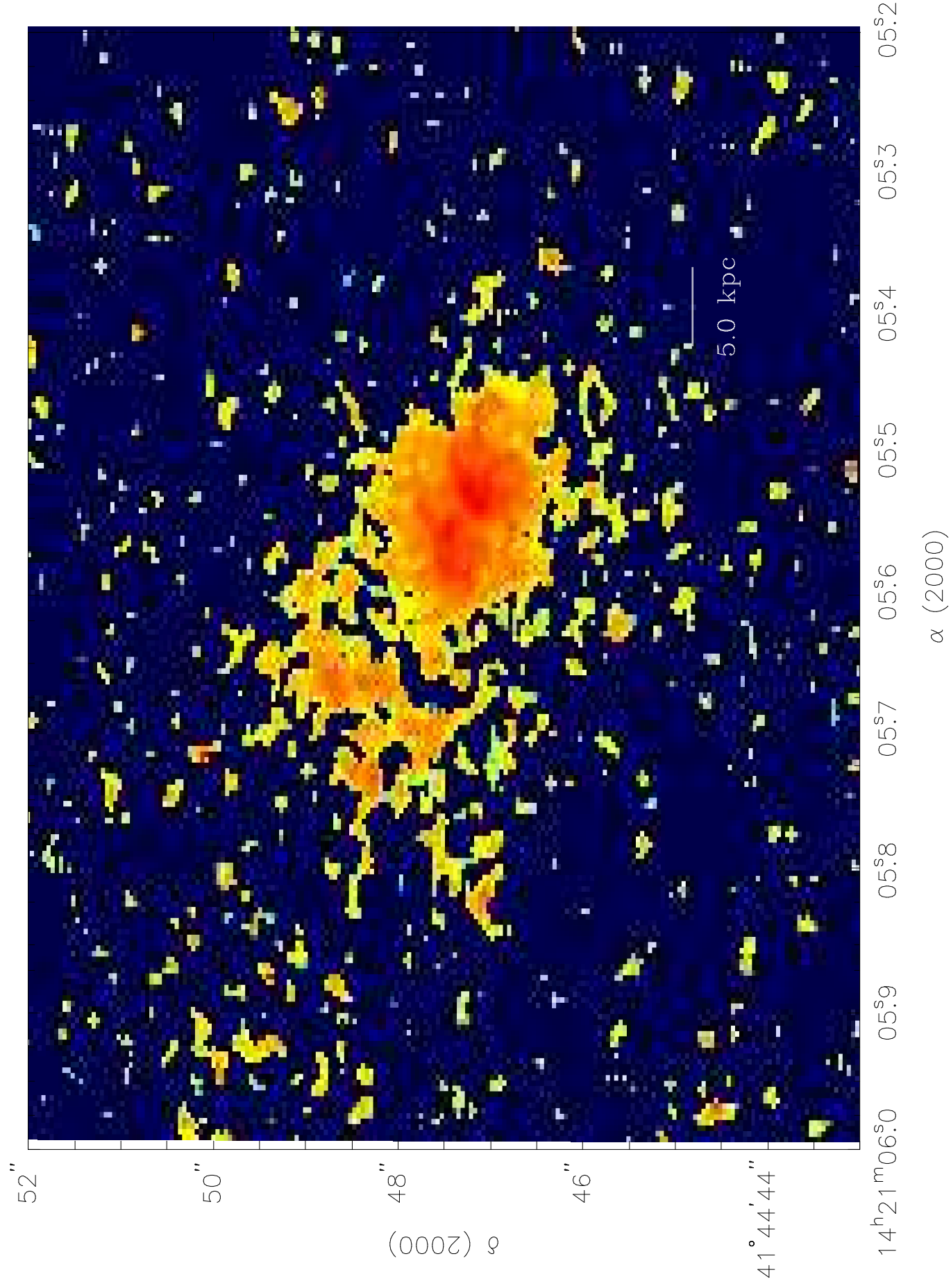
Table 2: Emission-line ratio

Distance from the nucleus arcsec	$\log(\text{He II } \lambda 4686/\text{H}\beta)$	$\log([\text{OIII}] \lambda 5007/\text{H}\beta)$
0	$-0.57 \pm 0.05$	$0.83 \pm 0.02$
0.7	$-0.60 \pm 0.04$	$0.79 \pm 0.02$
1.5	$-0.62 \pm 0.04$	$0.90 \pm 0.02$
2.2	$-0.66 \pm 0.05$	$0.87 \pm 0.02$
2.9	$-0.56 \pm 0.06$	$0.79 \pm 0.03$
3.6	$-0.60 \pm 0.08$	$0.83 \pm 0.03$

F702W FILTER (R)



F555W FILTER (V)



FR680N FILTER - [OIII] $\lambda$ 5007

